Supporting Information

Highly Active Chiral Oxazolinyl Aminophenolate Magnesium Initiators for Isoselective Ring-Opening Polymerization of *rac*-Lactide: Dinuclearity Induced Enantiomorphic Site Control

Jianwen Hu,[‡] Chao Kan,[‡] Haobing Wang* and Haiyan Ma*

Shanghai Key Laboratory of Functional Materials Chemistry and Laboratory of Organometallic Chemistry, School of Chemistry and Molecular Engineering, East China University of Science and Technology, 130 Meilong Road, Shanghai 200237, P. R. China

Contents

1. Experimental

1.1 Synthesis

1.1.1 General considerations

All manipulations were carried out under a dry argon atmosphere using standard Schlenk-line or glove-box techniques. Toluene and *n*-hexane were refluxed over sodium benzophenone ketyl prior to use. Benzene-d_6 and other reagents were properly dried and stored in a glove-box. $Mg[N(SiMe_3)_2]_2$ was synthesized according to the literature method.[S1] All other chemicals were commercially available and used after appropriate purification. NMR spectra were recorded on a Bruker AVANCE-400 spectrometer at 25 °C (^{1}H: 400 MHz; ^{13}C: 100 MHz) unless otherwise stated. Chemical shifts for ^{1}H and ^{13}C{^{1}H} NMR spectra were referenced internally using the residual solvent resonances and reported relative to tetramethylsilane (TMS). Elemental analyses were performed on an EA-1106 instrument.

1.1.2 Synthesis of proligands L^3H–L^6H

Synthesis of aminophenol ligands $\mathbf{L^{1,2}H}$ see our published result.[S2]

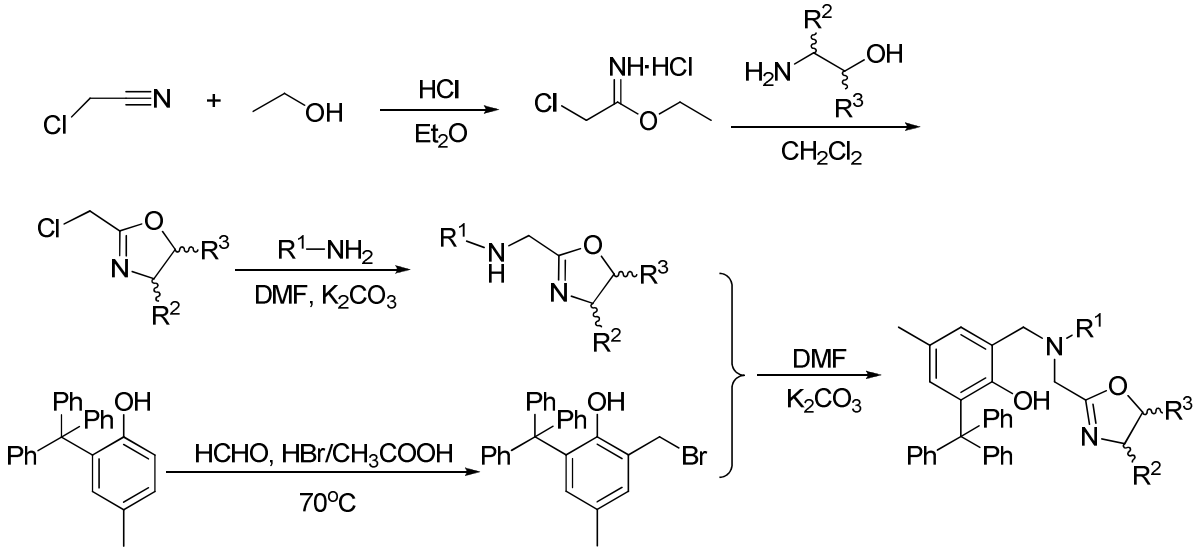

Scheme S1. Synthesis of proligands $\mathbf{L^{3–6}H}$.

1.1.2.1 Synthesis of (4-R^2-5-R^3-oxazolin-2-yl)methyl substituted secondary amines

2-Chloromethyl-4,5-substituted oxazoline[S3] (10 mmol) was dissolved in 20 mL of DMF, then the solution was slowly added to a mixture of excess primary amine (100 mmol) and K_2CO_3 (11 mmol) in about 10 h. The mixture was poured into water and extracted with ethyl acetate three times. The organic phase was dried over anhydrous $MgSO_4$. Evaporation of the solvent gave the target product as viscous oil with a purity of about 80%, which was used directly for the next step without further purification.

1.1.2.2 Synthesis of 2-{*N*-benzyl-*N*-[((3a*R*,8a*S*)-3a,8a-dihydro-8H-indeno[1,2-d]oxazolin-2-yl) methyl]aminomethyl}-4-methyl-6-(triphenylmethyl)phenol (L^3H)

2-Bromomethyl-4-methyl-6-(triphenylmethyl)phenol[S4] (3.99 g, 9.00 mmol) was added to a solution of crude *N*-benzyl-*N*-{[(3a*R*,8a*S*)- 3a,8a-dihydro-8H-indeno[1,2-d]oxazolin-2-yl]methyl}amine (3.13 g, ca. 9.00 mmol) and K_2CO_3 (1.37 g, 9.90 mmol) in 20 mL of DMF in 10 min. The mixture was stirred for 2 h, then it was poured into water and extracted with ethyl acetate three times. The organic phase was dried over anhydrous $MgSO_4$. Evaporation of the solvent gave viscous oil, which was purified by column chromatography (silica gel 200–300 Merck, petroleum ether/ethyl acetate/triethylamine = 25 : 1 : 0.01) to provide a white solid (2.77 g, 51%) after removal of all the volatiles. ^{1}H NMR ($CDCl_3$, 400 MHz, 298 K): δ 9.77 (br s, 1H, O*H*), 7.27–7.22 (m, 14H, Ar*H*), 7.20–7.14 (m, 8H, Ar*H*), 6.90 (d, 1H, ^4J = 1.6 Hz, ArH), 6.88–6.85 (m, 2H, Ar*H*), 6.75 (d, 1H, ^4J = 1.6 Hz, Ar*H*), 5.41 (d, 1H, ^3J = 8.0 Hz, C*H*N), 5.18–5.14 (m, 1H, C*H*O), 3.66 (d, 1H, ^2J = 13.2 Hz, ArCH_2), 3.56 (d, 1H, ^2J = 13.2 Hz, ArCH_2), 3.43 (s, 2H, PhCH_2), 3.30 (dd, 1H, ^2J = 18.4 Hz, ^3J = 6.8 Hz, CHCH_2), 3.09 (d, 1H, ^2J = 18.4 Hz, CHCH_2), 3.08 (d, 1H, ^2J = 15.6 Hz, NCH_2C=N), 3.00 (d, 1H, ^2J = 15.6 Hz, NCH_2C=N), 2.15 (s, 3H, ArCH_3). ^{13}C{^{1}H} NMR ($CDCl_3$, 100 MHz, 298 K): δ 164.5 (O*C*=N), 153.9, 146.3, 141.9, 139.5, 137.1, 134.0, 131.4, 131.3, 129.7, 129.6, 128.52, 128.47, 127.6, 127.4, 127.1, 126.6, 125.6, 125.4, 125.3, 122.4 (all Ar-*C*), 83.4 (*C*HN), 76.0 (*C*HO), 63.4 (Ph$_3$*C*), 58.1 (Ar*C*H$_2$), 56.6 (Ph*C*H$_2$), 49.0 (N*C*H$_2$C=N), 39.6 (CH*C*H$_2$), 21.0 (Ar*C*H$_3$). Anal. Calcd. for $C_{45}H_{40}N_2O_2$: C, 84.34; H, 6.29; N, 4.37. Found: C, 84.35; H, 6.14; N, 4.28%.

1.1.2.3 Synthesis of 2-{*N*-benzyl-*N*-[((4*S*,5*R*)-4,5-diphenyloxazolin-2-yl)methyl]aminomethyl}-4-methyl-6-(triphenylmethyl)phenol (L^4H)

The procedure was the same as that of **L^3H**, except that 2-bromomethyl-4-methyl-6-(triphenylmethyl)phenol (3.50 g, 7.90 mmol), crude *N*-benzyl-*N*-{[(4*S*,5*R*)-4,5-diphenyloxazolin-2-yl]methyl}amine (3.38 g, ca. 7.90 mmol), K_2CO_3 (1.20 g, 8.69 mmol) were used to provide **L^4H** as a white solid (3.11 g, 56%). ^{1}H NMR ($CDCl_3$, 400 MHz, 298 K): δ 9.88 (s, 1H, O*H*), 7.26–7.22 (m, 8H, Ar*H*), 7.21–7.11 (m, 10H, Ar*H*), 7.05–6.99 (m, 6H, Ar*H*), 6.98–6.94 (m, 3H, Ar*H*), 6.93–6.90 (m, 1H, Ar*H*), 6.88–6.78 (m, 4H, Ar*H*), 5.76 (d, 1H, ^3J = 10.3 Hz, C*H*N), 5.53 (d, 1H, ^3J = 10.3 Hz, C*H*O), 4.14 (d, 1H, ^2J = 13.6 Hz, PhCH_2), 4.09 (d, 1H, ^2J = 13.6 Hz, PhCH_2), 3.69 (s, 2H, ArCH_2), 3.42 (s, 2H, NCH_2C=N), 2.21 (s, 3H, ArCH_3). ^{13}C{^{1}H} NMR ($CDCl_3$, 100 MHz, 298 K): δ 165.1 (O*C*=N), 154.0, 146.2, 137.4, 136.9, 136.2, 134.2, 131.3, 130.0, 129.5, 128.6, 127.84, 127.83, 127.80, 127.56, 127.54, 127.13, 127.07, 127.02, 126.4, 125.5, 122.3 (all Ar-*C*), 85.2 (*C*HN), 73.9 (*C*HO), 63.4 (Ph$_3$*C*), 58.5 (Ar*C*H$_2$), 56.1 (N*C*H$_2$C=N), 48.3 (N*C*H$_2$Ph), 21.1 (Ar*C*H$_3$). Anal. Calcd. for $C_{50}H_{44}N_2O_2$: C, 85.19; H, 6.29; N, 3.97. Found: C, 85.02; H, 6.27; N, 3.92%.

1.1.2.4 Synthesis of (*R*)-2-{*N*-benzyl-*N*-[(4-phenyloxazolin-2-yl)methyl]aminomethyl}-4-methyl-6-(triphenylmethyl)phenol (L^5H)

The procedure was the same as that of $\mathbf{L^3H}$, except that 2-bromomethyl-4-methyl-6-(triphenylmethyl)phenol (4.99 g, 11.3 mmol), crude (*R*)-*N*-benzyl-*N*-[(4-phenyloxazolin-2-yl)methyl]amine (3.75 g, ca. 11.3 mmol), K_2CO_3 (1.71 g, 12.4 mmol) were used to provide $\mathbf{L^5H}$ as a white solid (3.17 g, 45%). ^{1}H NMR ($CDCl_3$, 400 MHz, 298 K): δ 9.84 (s, 1H, O*H*), 7.35–7.12 (m, 23H, Ar*H*), 6.94 (d, 1H, ^4J = 1.6 Hz, Ar*H*), 6.95–6.90 (m, 2H, Ar*H*), 6.86 (d, 1H, ^4J = 1.6 Hz, Ar*H*), 5.15 (*pseudo*-t, 1H, ^3J = 9.2 Hz, C*H*N), 4.52 (dd, 1H, ^3J = 10.0 Hz, ^2J = 8.4 Hz, CH_2O), 4.02 (*pseudo*-t, 1H, $^2J \approx {}^3J$ = 8.4 Hz, CH_2O), 3.92 (s, 2H, ArCH_2), 3.59 (d, 1H, ^2J = 12.8 Hz, PhCH_2), 3.54 (d, 1H, ^2J = 12.8 Hz, PhCH_2), 3.22 (s, 2H, NCH_2C=N), 2.19 (s, 3H, ArCH_3). ^{13}C{^{1}H} NMR ($CDCl_3$, 100 MHz, 298 K): δ 164.9 (O*C*=N), 153.9, 146.2, 142.0, 136.8, 134.2, 131.3, 131.2, 130.0, 129.4, 128.9, 128.5, 127.7, 127.5, 127.1, 126.9, 126.6, 125.4, 122.2 (all Ar-*C*), 74.4 (*C*HN), 69.5 (*C*H_2O), 63.4 (Ph$_3$*C*), 58.3 (Ar*C*H_2), 56.5 (Ph*C*H_2), 48.5 (N*C*H_2C=N), 21.0 (Ar*C*H_3). Anal. Calcd. for $C_{44}H_{40}N_2O_2$: C, 84.04; H, 6.41; N, 4.46. Found: C, 83.92; H, 6.50; N, 4.42%.

1.1.2.5 Synthesis of (*S*)-2-{*N*-benzyl-*N*-[(4-phenyloxazolin-2-yl)methyl]aminomethyl}-4-methyl-6-(triphenylmethyl)phenol (L^6H)

The procedure was the same as that of $\mathbf{L^3H}$, except that 2-bromomethyl-4-methyl-6-(triphenylmethyl)phenol (3.43 g, 7.73 mmol), crude (*S*)-*N*-^{n}butyl-*N*-[(4-phenyloxazolin-2-yl)methyl]amine (2.58 g, ca. 7.73 mmol), K_2CO_3 (1.17 g, 8.50 mmol) were used to provide $\mathbf{L^6H}$ as a white solid (3.17 g, 65%). ^{1}H NMR ($CDCl_3$, 400 MHz, 298 K): δ 9.84 (s, 1H, O*H*), 7.40–7.25 (m, 4H, Ar*H*), 7.24–7.15 (m, 16H, Ar*H*), 7.15–7.07 (m, 3H, Ar*H*), 6.95 (d, 1H, ^4J = 1.6 Hz, Ar*H*), 6.94–6.90 (m, 2H, Ar*H*), 6.85 (d, 1H, ^4J = 1.6 Hz, Ar*H*), 5.14 (*pseudo*-t, 1H, ^3J = 9.2 Hz, C*H*N), 4.50 (dd, 1H, ^3J = 10.0 Hz, ^2J = 8.4 Hz, CH_2O), 4.00 (*pseudo*-t, 1H, $^2J \approx {}^3J$ = 8.4 Hz, CH_2O), 3.91 (s, 2H, ArCH_2), 3.58 (d, 1H, ^2J = 12.8 Hz, PhCH_2), 3.53 (d, 1H, ^2J = 12.8 Hz, PhCH_2), 3.21 (s, 2H, NCH_2C=N), 2.18 (s, 3H, ArCH_3). ^{13}C{^{1}H} NMR ($CDCl_3$, 100 MHz, 298 K): δ 164.9 (O*C*=N), 153.9, 146.2, 142.0, 136.8, 134.2, 131.3, 131.2, 129.8, 129.4, 128.9, 128.5, 127.7, 127.5, 127.1, 126.9, 126.6, 125.4, 122.2 (all Ar-*C*), 74.4 (*C*HN), 69.5 (*C*H_2O), 63.4 (Ph$_3$*C*), 58.3 (Ar*C*H_2), 56.5 (Ph*C*H_2), 48.5 (N*C*H_2C=N), 21.0 (Ar*C*H_3). Anal. Calcd. for $C_{44}H_{40}N_2O_2$: C, 84.04; H, 6.41; N, 4.46. Found: C, 84.08; H, 6.35; N, 4.31%.

1.1.3 Synthesis of magnesium complexes

1.1.3.1 Synthesis of $[(L^1)MgN(SiMe_3)_2]$ (1)

In a glove box, the proligand $\mathbf{L^1H}$ (0.593 g, 1.00 mmol) was dissolved in toluene (3 mL) and was added dropwise to a solution of $Mg[N(SiMe_3)_2]_2$ (0.345 g, 1.00 mmol) in toluene (3 mL). The reaction

mixture was stirred at room temperature overnight, all the volatiles were removed under vacuum to afford a light yellow solid which was then recrystallized with a mixture of *n*-hexane and toluene. Colorless crystals of complex **1** were obtained in 48% (0.376 g). ^{1}H NMR (C_6D_6, 400 MHz, 298 K): δ 7.51 (d, 1H, ^{3}J = 8.0 Hz, Ar*H*), 7.46 (d, 6H, ^{3}J = 8.0 Hz, Ar*H*), 7.34 (d, 1H, ^{4}J = 2.2 Hz, Ar*H*), 7.13–7.00 (m, 5H × 0.9, toluene), 6.93 (m, 7H, Ar*H*), 6.88–6.79 (m, 2H, Ar*H*), 6.71–6.64 (m, 4H, Ar*H*), 4.33 (d, 1H, ^{2}J = 12.4 Hz, ArCH_2), 3.77 (d, 1H, ^{2}J =18.4 Hz, NCH_2C=N), 2.97 (d, 1H, ^{2}J =12.4 Hz, ArCH_2), 2.95 (d, 1H, ^{2}J =18.4 Hz, NCH_2C=N), 2.36–2.27 (m, 1H, NC*H* of cyclohexyl), 2.23 (s, 3H, ArCH_3), 2.10 (s, 3H × 0.9, toluene), 2.08–2.01 (m, 1H, CH_2 of cyclohexyl), 1.75–1.67 (m, 1H, CH_2 of cyclohexyl), 1.56–1.48 (m, 2H, CH_2 of cyclohexyl), 1.38–1.31 (m, 1H, CH_2 of cyclohexyl), 1.24–1.20 (m, 1H, CH_2 of cyclohexyl), 1.11–0.97 (m, 2H, CH_2 of cyclohexyl), 0.87–0.79 (m, 2H, CH_2 of cyclohexyl), 0.29 (s, 18H, N(Si(CH_3)$_3$)$_2$). ^{13}C{^{1}H} NMR (C_6D_6, 100 MHz, 298 K): δ 169.6 (O*C*=N), 163.5, 150.9, 147.8, 137.9 (toluene), 137.1, 136.7, 133.6, 131.7, 131.6, 129.3 (toluene), 128.6 (toluene), 127.0, 126.4, 125.7 (toluene), 125.6, 125.1, 121.6, 121.1, 120.7, 110.9 (All Ar-*C*), 65.0 (Ph_3C), 64.1 (ArCH_2), 56.6 (N*C*H), 45.0 (NCH_2C=N), 32.0 (*C*H_2), 29.3 (*C*H_2), 27.5 (*C*H_2), 26.1 (*C*H_2), 25.77 (*C*H_2), 25.74 (*C*H_2), 23.1 (*C*H_2), 21.5 (Ar*C*H_3), 21.1 (toluene), 6.71 (N(Si(*C*H_3)$_3$)$_2$). Anal. Calcd. for $C_{47}H_{55}MgN_3O_2Si_2$·0.9 C_7H_8: C, 74.49; H, 7.53; N, 4.89. Found: 74.21; H, 7.25; N, 4.35%.

1.1.3.2 Synthesis of [(L^2)MgN($SiMe_3$)$_2$] (2)

The procedure was the same as that of complex **1**, except that **L^2H** (0.607 g, 1.00 mmol) and Mg[N($SiMe_3$)$_2$]$_2$ (0.345 g, 1.00 mmol) were used to afford complex **2** as colorless solids (0.300 g, 38%). ^{1}H NMR (C_6D_6, 400 MHz, 298 K): two isomers (**Mg2a** : **Mg2b** = 10 : 1), **Mg2a**: δ 7.70 (d, 6H, ^{3}J = 7.6 Hz, Ar*H*), 7.50 (d, 1H, ^{4}J = 2.0 Hz, Ar*H*), 7.45 (d, 1H, ^{3}J = 7.5 Hz, Ar*H*), 7.12 (t, 6H, ^{3}J = 7.6 Hz, Ar*H*), 6.97 (t, 1H, ^{3}J = 7.6 Hz, Ar*H*), 6.86 (t, 3H, ^{3}J = 7.3 Hz, Ar*H*), 6.77 (d, 1H, ^{3}J = 7.8 Hz, Ar*H*), 6.69 (d, 1H, ^{4}J = 2.0 Hz, Ar*H*), 4.19 (*pseudo*-t, 1H, ^{3}J = 6.8 Hz, C*H*O), 4.14 (d, 1H, ^{2}J = 12.0 Hz, ArCH_2), 3.12 (d, 1H, ^{3}J = 7.6 Hz, C*H*N), 2.75 (d, 1H, ^{2}J = 16.8 Hz, NCH_2C=N), 2.69 (d, 1H, ^{2}J = 18.0 Hz, CHCH_2), 2.53 (dd, 1H, ^{2}J = 18.0 Hz, ^{3}J = 6.8 Hz, CHCH_2), 2.50 (d, 1H, ^{2}J = 12.0 Hz, ArCH_2), 2.31 (s, 3H, ArCH_3), 2.27–2.22 (m, 2H, NCH_2C=N and NCH_2), 2.15–2.07 (m, 1H, NCH_2), 1.33–1.22 (m, 1H, NCH$_2$CH_2), 1.21–1.09 (m, 1H, NCH$_2$CH_2), 1.01–0.87 (m, 2H, CH_2CH$_3$), 0.70 (t, 3H, ^{3}J = 7.2 Hz, CH$_2$CH_3), 0.26 (s, 18H, N(Si(CH_3)$_3$)$_2$). ^{13}C{^{1}H} NMR (C_6D_6, 100 MHz, 298 K): δ 172.3 (O*C*=N), 164.4, 148.0, 139.5, 138.6, 135.1, 133.6, 131.8, 131.6, 130.9, 129.2, 127.4, 127.3, 125.2, 125.1, 121.7, 120.4 (all Ar-*C*), 88.2 (*C*HN), 71.1 (*C*HO), 64.1 (Ph_3C), 62.0 (ArCH_2), 60.0 (N*C*H$_2$C=N), 51.0 (N*C*H$_2$CH$_2$), 38.0 (CH*C*H$_2$), 28.3 (NCH$_2$*C*H$_2$), 21.2 (Ar*C*H$_3$), 20.8 (*C*H$_2$CH$_3$), 13.9 (CH$_2$*C*H$_3$), 6.41 (N(Si(*C*H$_3$)$_3$)$_2$). Anal. Calcd. for $C_{48}H_{59}MgN_3O_2Si_2$: C, 72.93; H, 7.52; N, 5.32. Found: C, 72.82; H, 7.57; N, 5.21%.

1.1.3.3 Synthesis of [(L^3)MgN($SiMe_3$)$_2$] (3)

The procedure was the same as that of complex **1**, except that $\mathbf{L^3H}$ (0.641 g, 1.00 mmol) and Mg[N($SiMe_3$)$_2$]$_2$ (0.345 g, 1.00 mmol) were used to afford complex **3** as colorless crystals (0.333 g, 40%). ^{1}H NMR (C_6D_6, 400 MHz, 298 K): two isomers (**Mg3a** : **Mg3b** = 14 : 1), **Mg3a**: δ 7.73 (d, 6H, ^3J = 7.6 Hz, Ar*H*), 7.49 (d, 1H, ^4J = 2.0 Hz, Ar*H*), 7.39 (d, 1H, ^3J = 7.6 Hz, Ar*H*), 7.18 (t, 1H, ^3J = 7.6 Hz, ArH), 7.12 (t, 6H, ^3J = 7.6 Hz, Ar*H*), 7.06–6.95 (m, 4H, Ar*H*), 6.87–6.80 (m, 5H, Ar*H*), 6.77 (d, 1H, ^3J = 7.6 Hz, Ar*H*), 6.32 (d, 1H, ^4J = 2.0 Hz, Ar*H*), 4.06–4.02 (m, 2H, C*H*N and C*H*O), 3.95 (d, 1H, ^2J = 14.0 Hz, PhCH_2), 3.73 (d, 1H, ^2J = 14.0 Hz, PhCH_2), 2.88–2.82 (m, 3H, 2H of ArCH_2 and 1H of NCH_2C=N), 2.65 (d, 1H, ^2J = 18.3 Hz, CHCH_2), 2.54 (d, 1H, ^2J = 16.4 Hz, NCH_2C=N), 2.50 (dd, 1H, ^2J = 18.3 Hz, ^3J = 6.4 Hz, CHCH_2), 2.17 (s, 3H, ArCH_3), 0.32 (s, 18H, N(Si(CH_3)$_3$)$_2$). ^{13}C{^{1}H} NMR (C_6D_6, 100 MHz, 298 K): δ 172.0 (O*C*=N), 164.7, 148.0, 139.5, 138.7, 134.6, 133.5, 132.0, 131.9, 131.52, 131.46, 130.8, 129.3, 128.9, 128.8, 127.3, 125.23, 125.15, 121.4, 120.4 (all Ar-*C*), 88.2 (*C*HN), 70.8 (*C*HO), 64.1 (Ph$_3$*C*), 61.8 (Ar*C*H$_2$), 60.8 (Ph*C*H$_2$), 49.7 (N*C*H$_2$C=N), 38.0 (CH*C*H$_2$), 21.0 (Ar*C*H$_3$), 6.45 (N(Si(*C*H$_3$)$_3$)$_2$). Anal. Calcd. for $C_{51}H_{57}MgN_3O_2Si_2$: C, 74.29; H, 6.97; N, 5.10. Found: C, 74.02; H, 6.92; N, 5.17%.

1.1.3.4 Synthesis of [(L^4)MgN($SiMe_3$)$_2$] (4)

The procedure was the same as that of complex **1**, except that $\mathbf{L^4H}$ (0.705 g, 1.00 mmol) and Mg[N($SiMe_3$)$_2$]$_2$ (0.345 g, 1.00 mmol) were used to afford complex **4** as light yellow crystals (0.393 g, 44%). ^{1}H NMR (C_6D_6, 400 MHz, 298 K): two isomers (**Mg4a** : **Mg4b** = 10 : 1), **Mg4a**: δ 7.77 (d, 6H, ^3J = 7.6 Hz, Ar*H*), 7.56 (s, 1H, Ar*H*), 7.53 (d, 1H, ^3J = 7.6 Hz, Ar*H*), 7.19 (t, 6H, ^3J = 7.6 Hz, Ar*H*), 7.13–7.04 (m, 5H × 0.6, toluene), 7.03–6.95 (m, 6H, Ar*H*), 6.90–6.75 (m, 7H, Ar*H*), 6.62–6.51 (m, 4H, Ar*H*), 6.45 (s, 1H, Ar*H*), 4.26 (d, 1H, ^3J = 8.6 Hz, C*H*N), 4.21 (d, 1H, ^2J = 11.6 Hz, ArCH_2), 4.08 (d, 1H, ^2J = 13.6 Hz, PhCH_2), 3.90 (d, 1H, ^2J = 13.6 Hz, PhCH_2), 3.40 (d, 1H, ^2J = 15.6 Hz, NCH_2C=N), 3.13 (d, 1H, ^3J = 8.6 Hz, C*H*O), 2.90 (d, 1H, ^3J = 11.6 Hz, ArCH_2), 2.80 (d, 1H, ^2J = 15.6 Hz, NCH_2C=N), 2.10 (s, 3H × 0.6, toluene), 2.09 (s, 3H, ArCH_3), 0.19 (s, 18H, N(Si(CH_3)$_3$)$_2$). ^{13}C{^{1}H} NMR (C_6D_6, 100 MHz, 298 K): δ 174.5 (O*C*=N), 165.2, 148.2, 137.9 (toluene), 134.6, 134.5, 133.3, 133.2, 132.4, 131.8, 131.6, 131.4, 130.9, 129.3 (toluene), 129.1, 129.0, 128.6 (toluene), 127.5, 127.3, 126.5, 125.7 (toluene), 125.3, 121.1, 120.7 (all Ar-*C*), 90.3 (*C*HN), 67.7 (*C*HO), 63.9 (Ph$_3$*C*), 62.2 (Ar*C*H$_2$), 61.6 (Ph*C*H$_2$), 50.0 (N*C*H$_2$C=N), 21.4 (toluene), 20.8 (Ar*C*H$_3$) 6.49 N(Si(*C*H$_3$)$_3$)$_2$). Anal. Calcd. for $C_{56}H_{61}N_3O_2Si_2Mg \cdot 0.6\ C_7H_8$: C, 76.60; H, 7.03; N, 4.45. Found: C,76.57; H, 7.16; N, 4.17%.

1.1.3.5 Synthesis of [(L^5)MgN($SiMe_3$)$_2$] (5)

The procedure was the same as that of complex **1**, except that $\mathbf{L^5H}$ (0.629 g, 1.00 mmol) and Mg[N($SiMe_3$)$_2$]$_2$ (0.345 g, 1.00 mmol) were used to afford complex **5** as light yellow crystals (0.468 g,

58%). ^{1}H NMR (C_6D_6, 400 MHz, 298 K): two isomers (**Mg5a** : **Mg5b** = 4 : 1). Although the percentage of isomer **Mg5b** is relatively large in this case, due to serious overlapping of most signals with those of **Mg5a**, the NMR signals of **Mg5b** could not be identified completely, thus only the NMR data of **Mg5a** are listed: δ 7.64 (d, 6H, ^3J = 7.6 Hz, Ar*H*), 7.42 (s, 1H, Ar*H*), 7.12–6.86 (m, 19H, Ar*H*), 6.38 (s, 1H, Ar*H*), 4.16 (d, 1H, ^2J = 12.0 Hz, ArCH_2), 4.00 (d, 1H, ^2J = 14.0 Hz, PhCH_2), 3.91 (d, 1H, ^2J = 14.0 Hz, PhCH_2), 3.64–3.61 (m, 1H, C*H*N), 3.39–3.21 (m, 2H, CH_2O and ArCH_2), 3.04–2.96 (m, 2H, CH_2O and NCH_2C=N), 2.76 (d, 1H, ^2J = 16.8 Hz, NCH_2C=N), 2.14 (s, 3H, ArCH_3), 0.17 (s, 18H, N(Si(CH_3)$_3$)$_2$). ^{13}C{^{1}H} NMR (C_6D_6, 100 MHz, 298 K): δ 173.1 (O*C*=N), 164.5, 148.0, 139.3, 135.2, 133.6, 131.84, 131.81, 131.7, 131.1, 129.3, 129.2, 128.99, 128.96, 128.64, 128.57, 127.3, 126.9, 125.2, 121.0, 120.4 (all Ar-*C*), 77.3 (*C*HN), 64.3 (*C*H_2O), 64.0 (Ph$_3$*C*), 61.1 (Ar*C*H_2), 60.4 (Ph*C*H_2), 48.2 (N*C*H_2C=N), 21.0 (Ar*C*H_3), 6.34 (N(Si(*C*H_3)$_3$)$_2$). Anal. Calcd. for $C_{50}H_{57}MgN_3O_2Si_2$·0.1 C_7H_8: C, 74.11; H, 7.09; N, 5.11. Found: C, 73.55; H, 7.17; N, 4.87%.

1.1.3.6 Synthesis of [(L^6)MgN(SiMe$_3$)$_2$] (6)

The procedure was the same as that of complex **1**, except that **L^{6}H** (0.377 g, 0.60 mmol) and Mg[N(SiMe$_3$)$_2$]$_2$ (0.207 g, 0.60 mmol) were used to afford complex **6** as light yellow solids (0.276 g, 57%). ^{1}H NMR (C_6D_6, 400 MHz, 298 K): two isomers (**Mg6a** : **Mg6b** = 4 : 1). Although the percentage of isomer **Mg6b** is relatively large in this case, due to serious overlapping of most signals with those of **Mg6a**, the NMR signals of **Mg6b** could not be identified completely, thus only the NMR data of **Mg6a** are listed: δ 7.64 (d, 6H, ^3J = 7.6 Hz, Ar*H*), 7.42 (d, 1H, ^4J = 2.2 Hz, Ar*H*), 7.14–7.07 (m, 13H, Ar*H*), 7.07–7.00 (m, 4H, Ar*H*), 7.00–6.95 (m, 2H, Ar*H*), 6.38 (d, 1H, ^4J = 2.2 Hz, Ar*H*), 4.16 (d, 1H, ^2J = 12.0 Hz, ArCH_2), 4.00 (d, 1H, ^2J = 14.0 Hz, PhCH_2), 3.92 (d, 1H, ^2J = 14.0 Hz, PhCH_2), 3.65–3.60 (m, 1H, C*H*N), 3.34–3.20 (m, 2H, CH_2O and ArCH_2), 3.03 (d, 1H, ^2J = 16.8 Hz, NCH_2C=N), 2.98 (d, 1H, ^2J = 12.0 Hz, CH_2O), 2.77 (d, 1H, ^2J = 16.8 Hz, NCH_2C=N), 2.15 (s, 3H, ArCH_3), 0.17 (s, 18H, N(Si(CH_3)$_3$)$_2$). ^{13}C{^{1}H} NMR (C_6D_6, 100 MHz, 298 K): δ 173.1 (O*C*=N), 164.5, 148.0, 139.4, 135.2, 133.6, 131.85, 131.81, 131.7, 131.1, 129.3, 129.1, 129.0, 128.96, 128.64, 128.57, 127.3, 126.9, 125.2, 121.0, 120.4 (all Ar-*C*), 77.3 (*C*HN), 64.3 (*C*H_2O), 64.0 (Ph$_3$*C*), 61.1 (Ar*C*H_2), 60.4 (Ph*C*H_2), 48.3 (N*C*H_2C=N), 21.0 (Ar*C*H_3), 6.35 (N(Si(*C*H_3)$_3$)$_2$). Anal. Calcd. for $C_{50}H_{57}MgN_3O_2Si_2$·0.07 C_7H_8: C, 74.05; H, 7.08; N, 5.13. Found: C, 73.33; H, 7.39; N, 4.68%.

1.2 *X*-ray diffraction measurements

Single crystals of complexes **1**, **3**, **5** and **6** were obtained by recrystallization with a mixture of toluene and *n*-hexane respectively at room temperature. The X-ray diffraction measurements were

performed on a Bruker SMART APEX II diffractometer with graphite-monochromated Mo-Kα (λ= 0.71073 Å) radiation. The data of complexes **1**, **3**, **5** and **6** were collected using ω-scan techniques. All structures were solved by direct methods and refined using Fourier techniques. An absorption correction based on SADABS was applied.[S5] All non-hydrogen atoms were refined by full-matrix least-squares on F^2 using the SHELXTL program package.[S6] Hydrogen atoms were located and refined by the geometry method. The cell refinement, data collection, and reduction were done by Bruker SAINT.[S7] The structure solution and refinement were performed by SHELXS-97[S8] and SHELXL-97[S9] respectively. For further crystal data and details of measurements see Table S1. Molecular structures were generated using ORTEP program.[S10] CCDC numbers 1840380-1840383, contain the supplementary crystallographic data for this paper. These data can be obtained free of charge from the Cambridge Crystallographic Data Centre via www.ccdc.cam.ac.uk/data_request/cif.

1.3 Ring-opening polymerization of *rac*-lactide

1.3.1 General considerations

rac-Lactide was recrystallized with dry toluene and then sublimed twice under vacuum at 90 °C. 2-Propanol was dried over calcium hydride prior to distillation. Glassware and vials used in the polymerization were dried in an oven at 120 °C overnight and exposed to vacuum-argon cycle three times. Gel permeation chromatography (GPC) analyses were carried out on a Agilent 1260 infinity instrument in THF at 25 °C, at a flow rate of 1 mL·min^{-1}, with two PL gel 5μm Mixed-C columns (7.5 × 300 mm). Calibration standards were commercially available narrowly distributed linear polystyrene samples that cover a broad range of molar masses ($10^3 < M_n < 7.0\times10^5$ g·mol^{-1}). Differential scanning calorimetry (DSC) measurements were obtained on a Perkin Elmer Jade differential scanning calorimeter and the instrument was calibrated using zinc and indium standards. Melting points (T_m) of the polymer samples were determined from the second heating cycles with a heating/cooling rate of 5 °C/min under nitrogen atmosphere (20 mL/min). DSC data were analyzed using Pyris V9.0.2 software. The reported T_m values are the average of three runs; all of the individual runs were from the second heating cycles of fresh PLA samples.

Monomer conversion determination was monitored by integration of monomer *vs.* polymer methine resonances in the ^{1}H NMR spectra. All spectroscopic analyses of polymers and homonuclear decoupled

^{1}H NMR spectra were performed in $CDCl_3$ on a Bruker Avance 400 MHz spectrometer with a cryoprobe.

1.3.2 Typical polymerization procedure

In a glove box, an initiator solution (0.5 mL, 10 mmol/mL) from a stock solution in toluene or THF was injected respectively to a series of 10 mL Schlenk tubes loaded with *rac*-lactide (0.144 g, 1.0 mmol) and suitable amount (0.5 mL) of the same dry solvent. Then, each Schlenk tube was taken out of the glove box and immersed quickly in an oil bath thermostatted at 25 °C. The mixture was stirred and quenched at the specific time interval by adding an excess amount of normal light petroleum ether. After being dissolved with dichloromethane, a small amount of aliquot of the bulk solution was withdrawn and dried under reduced pressure for monomer conversion determination via ^{1}H NMR spectroscopy. The bulk solution was slightly concentrated and the polymer was precipitated from dichloromethane via the addition of excess methanol. The collected polymer sample was further dried in a vacuum oven at 60 °C for 16 h to constant weight for gel permeation chromatography (GPC), ^{1}H and homonuclear decoupled ^{1}H NMR analyses.

In the cases where 2-propanol was used, the monomer solution was treated first with the solution of 2-propanol for 5 min, and then the solution of initiator was injected to the mixture. Otherwise the procedures were the same.

In the cases where the polymerization run was carried out at low temperature (−40 ºC), the initiator solution and some dry solvent were pre-cooled to −40 ºC in the refrigerator of the glovebox respectively. Upon the injection of the catalyst solution into to the solution (or mixture) of monomer in the cold solvent, the Schlenk tube was brought out of the glovebox and quickly immersed into a cold bath preset at the desired temperature. Otherwise the procedures were the same.

1.3.3 DOSY experiments

DOSY experiments were carried out on a Bruker AVANCE-400 spectrometer equipped with a BBFO-z-atm probe having actively shielded z-gradient coil. Diffusion ordered NMR data were acquired using the Bruker pulse program ledbpgp2s1d employing a double stimulated echo with three spoiling gradients. Sine-shaped gradient pulses were used with typical durations (P30) from 3.00 to 3.30 ms for ^{1}H

together with a diffusion period of 20 ms (D20). Gradient recovery delays of 200 μs were applied after each gradient pulse. Data were systematically accumulated by linearly varying the diffusion encoding gradients over a range from 2% to 95% for 64 gradient increment values. The signal decay dimension on the pseudo-2D data was generated by Fourier transformation of the time-domain data. DOSY plots were generated by using the DOSY processing module of TopSpin. Parameters were optimized empirically to find the best quality of data for presentation purposes. Translational diffusion coefficients (D_t) were calculated by fitting intensity data to the Stejskal-Tanner expression.

2. Results

2.1 X-ray molecular structures

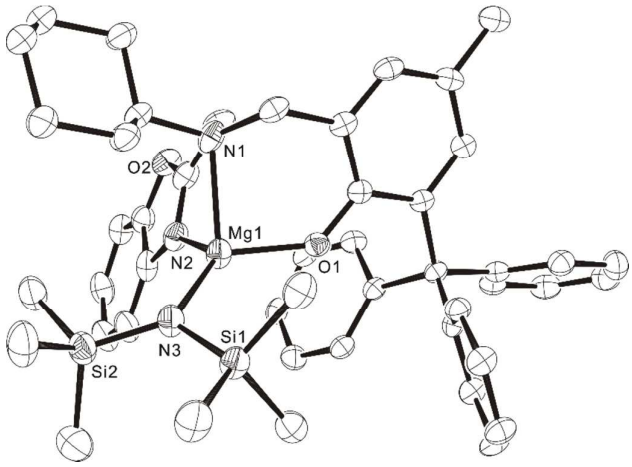

Figure S1. X-ray molecular structure of **1**. Thermal ellipsoids represent the 50% probability surfaces. Hydrogen atoms are omitted for the sake of clarity. Selected bond lengths (Å) and angles (°): Mg1–O1 1.896(2), Mg1–N1 2.230(3), Mg1–N2 2.122(2), Mg1–N3 1.990(2), O1–Mg1–N1 88.47(9), O1–Mg1–N2 107.51(9), O1–Mg1–N3 123.81(10), N1–Mg1–N2 79.57(9), N1–Mg1–N3 126.28(10), N2–Mg1–N3 120.04(10).

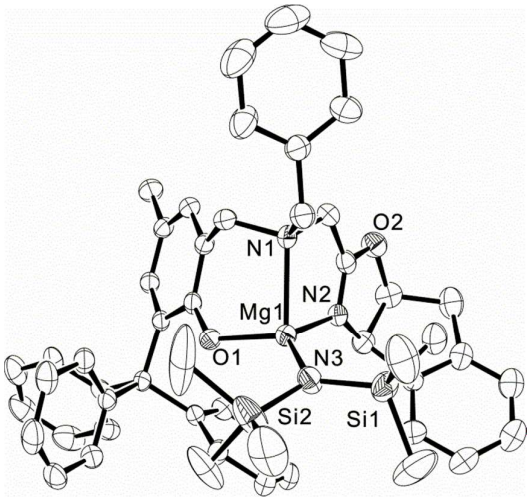

Figure S2. X-ray molecular structure of **3**. Thermal ellipsoids represent the 50% probability surfaces. Hydrogen atoms are omitted for the sake of clarity. Selected bond lengths (Å) and angles (°): Mg1–O1 1.899(4), Mg1–N1 2.221(4), Mg1–N2 2.107(5), Mg1–N3 1.972(4), O1–Mg1–N1 94.77(16), O1–Mg1–N2 103.52(17), O1–Mg1–N3 122.93(18), N1–Mg1–N2 79.17(18), N1–Mg1–N3 116.17(19), N2–Mg1–N3 127.55(19).

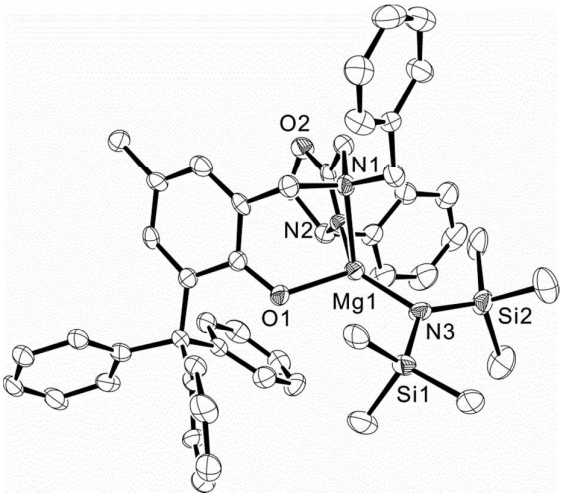

Figure S3. *X*-ray molecular structure of **5**. Thermal ellipsoids represent the 50% probability surfaces. Hydrogen atoms are omitted for the sake of clarity. Selected bond lengths (Å) and angles (°): Mg1–O1 1.923(5), Mg1–N1 2.202(6), Mg1–N2 2.120(6), Mg1–N3 1.974(6), O1–Mg1–N1 96.2(2), O1–Mg1–N2 100.9(2), O1–Mg1–N3 119.6(2), N1–Mg1–N3 111.9(3), N2–Mg1–N3 135.3(2), N1–Mg1–N2 79.1(2).

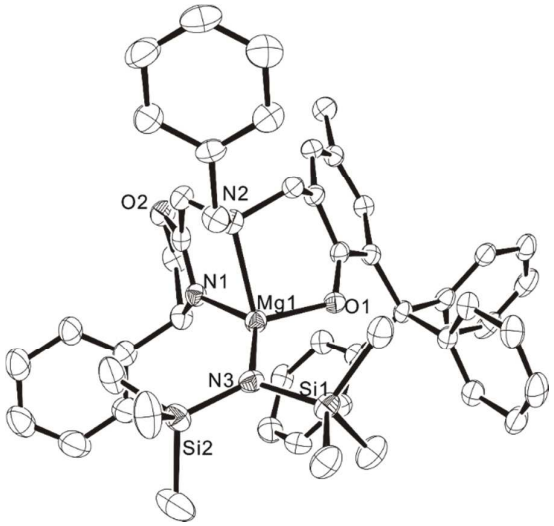

Figure S4. X-ray molecular structure of **6**. Thermal ellipsoids represent the 50% probability surfaces. Hydrogen atoms are omitted for the sake of clarity. Selected bond lengths (Å) and angles (°): Mg1–O1 1.916(2), Mg1–N1 2.123(3), Mg1–N2 2.209(3), Mg1–N3 1.980(3), O1–Mg1–N1 100.67(11), O1–Mg1–N2 96.39(11), O1–Mg1–N3 119.80(12), N1–Mg1–N2 78.94(11), N1–Mg1–N3 135.49(12), N2–Mg1–N3 111.55(12).

Table S1. Crystallographic data for **1**, **3**, **5** and **6**.

	1	**3**	**5**	**6**
Empirical formula	$C_{47}H_{57}MgN_3O_2Si_2$	$C_{51}H_{57}MgN_3O_2Si_2$	$C_{50}H_{57}MgN_3O_2Si_2$	$C_{50}H_{57}MgN_3O_2Si_2$
Formula weight	776.45	824.48	858.54	812.48
Temp (K)	133(2)	296(2)	130	130
Crystal size (mm)	0.21 × 0.17 × 0.13	0.22 × 0.17 × 0.13	0.25 × 0.15 × 0.05	0.15 × 0.10 × 0.05
Crystal system	Monoclinic	Orthorhombic	Monoclinic	Monoclinic
Space group	P 21/c	P 21 21 21	C 1 2 1	C 1 2 1
a (Å)	15.801(2)	11.371(4)	22.132(5)	22.162(3)
b (Å)	13.976(18)	19.871(7)	11.214(3)	11.233 (13)
c (Å)	13.976(18)	20.675(7)	19.876(5)	19.873(3)
α (°)	90	90	90	90
β (°)	13.976(18)	90	98.636(4)	98.551(5)
γ (°)	90	90	90	90
Volume ($Å^3$)	4342.3(10)	4671(3)	4877(2)	4892.2(12)
Z	4	4	4	4
Density $_{calcd}$ (Mg/m^3)	1.188	1.172	1.169	1.166
Abs coeff (mm^{-1})	0.137	0.131	0.128	0.128
F (000)	1664	1760	1836	1836
θ range (°)	1.788 to 26.000	1.421 to 25.499	1.036 to 30.412	1.858 to 30.386
Data collected (*hkl*)	−17 to 19, ±17, ±24	±13, ±24, −25 to 22	−31 to 23, ±15, ±28	−31 to 31, −14 to 15, −26 to 28
Reflns collected/unique	31254 / 8546	32852 / 8688	24079 / 12718	24531 / 11794
R(int)	0.0952	0.1041	0.1640	0.0686
Max. and min. transmn	0.7456, 0.6365	0.7456, 0.6298	0.7460, 0.5972	0.7461, 0.5299
Data/restrains/para	8546 / 72 / 557	8688 / 6 / 550	12718 / 1 / 564	11794 / 1 / 564
Goodness-of-fit on F^2	1.003	0.985	0.907	0.941
Final R_1, wR_2 [I > 2σ(I)]	0.0520, 0.1023	0.0538, 0.0969	0.0751, 0.1181	0.0497, 0.0805
R_1 , wR_2 (all data)	0.1123, 0.1285	0.1367, 0.1251	0.2477, 0.1824	0.1342, 0.1039
$\Delta\rho_{max,\ min}$ (e $Å^{-3}$)	0.324, −0.291	0.272, −0.328	0.333, −0.363	0.274, −0.418

2.2 ^{1}H NMR and ^{13}C{^{1}H} NMR Spectra of Complexes 1-6

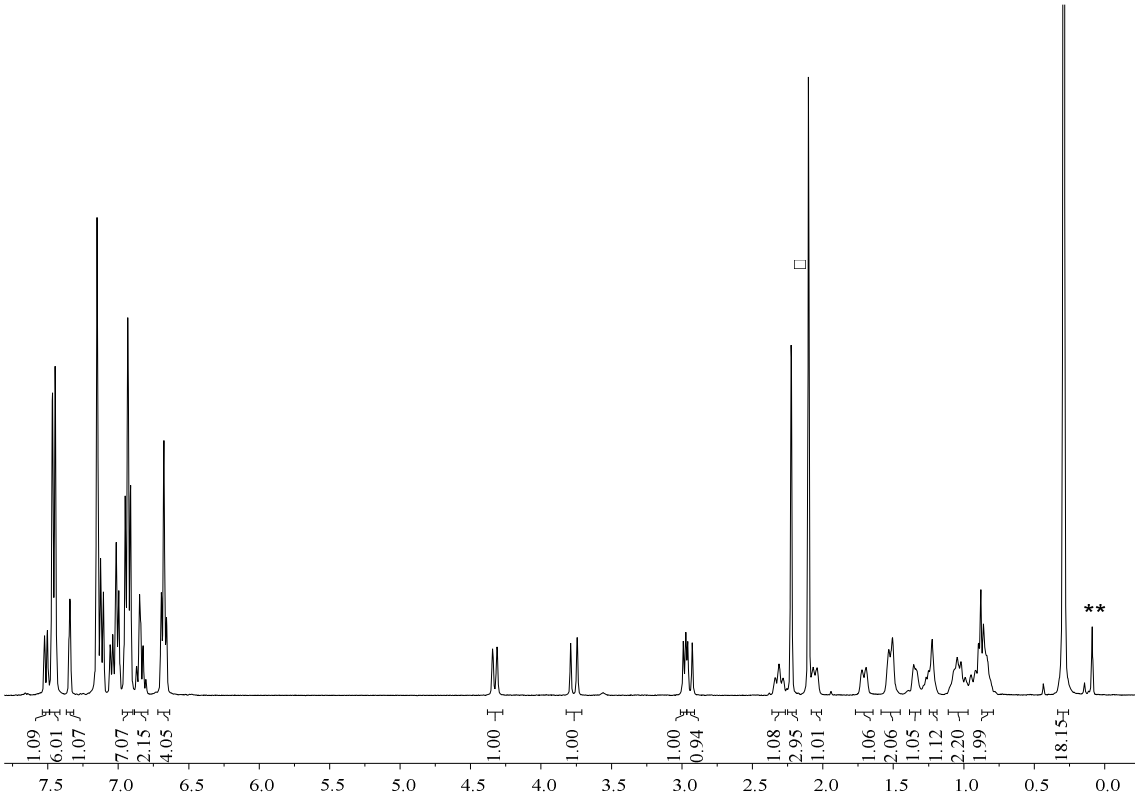

Figure S5. ^{1}H NMR spectrum of complex **1** (400 MHz, C_6D_6, 25 °C). (□: methyl signal of residual toluene; **: free $HN[Si(CH_3)_2]_2$).

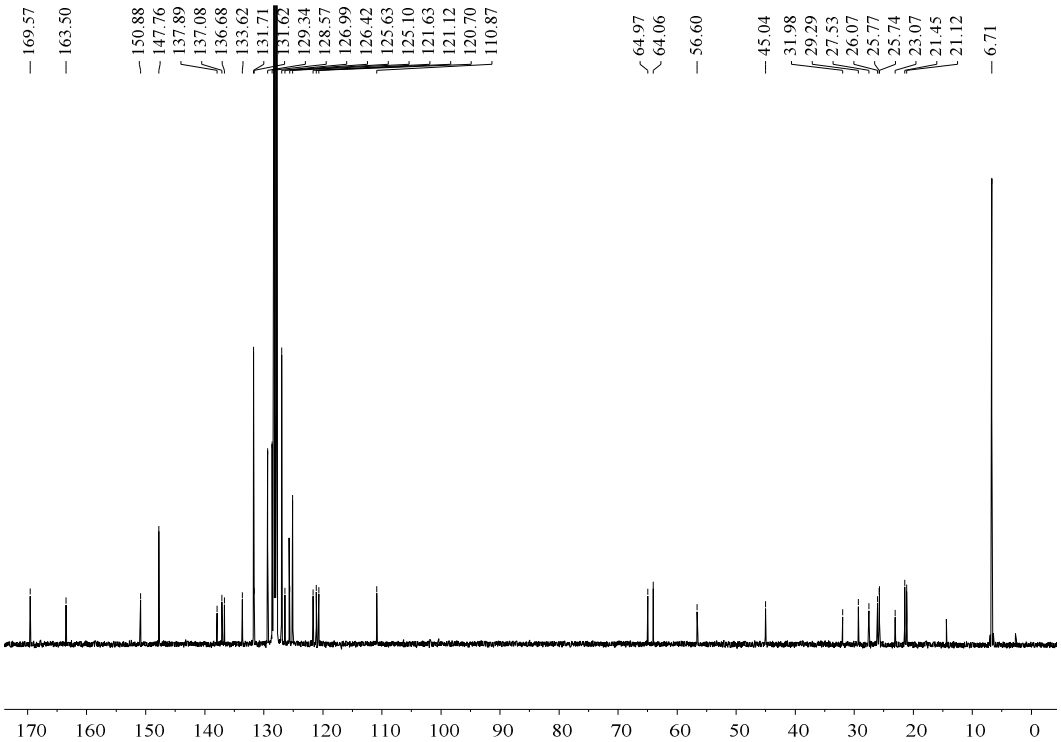

Figure S6. ^{13}C{^{1}H} NMR spectrum of complex **1** (100 MHz, C_6D_6, 25 °C).

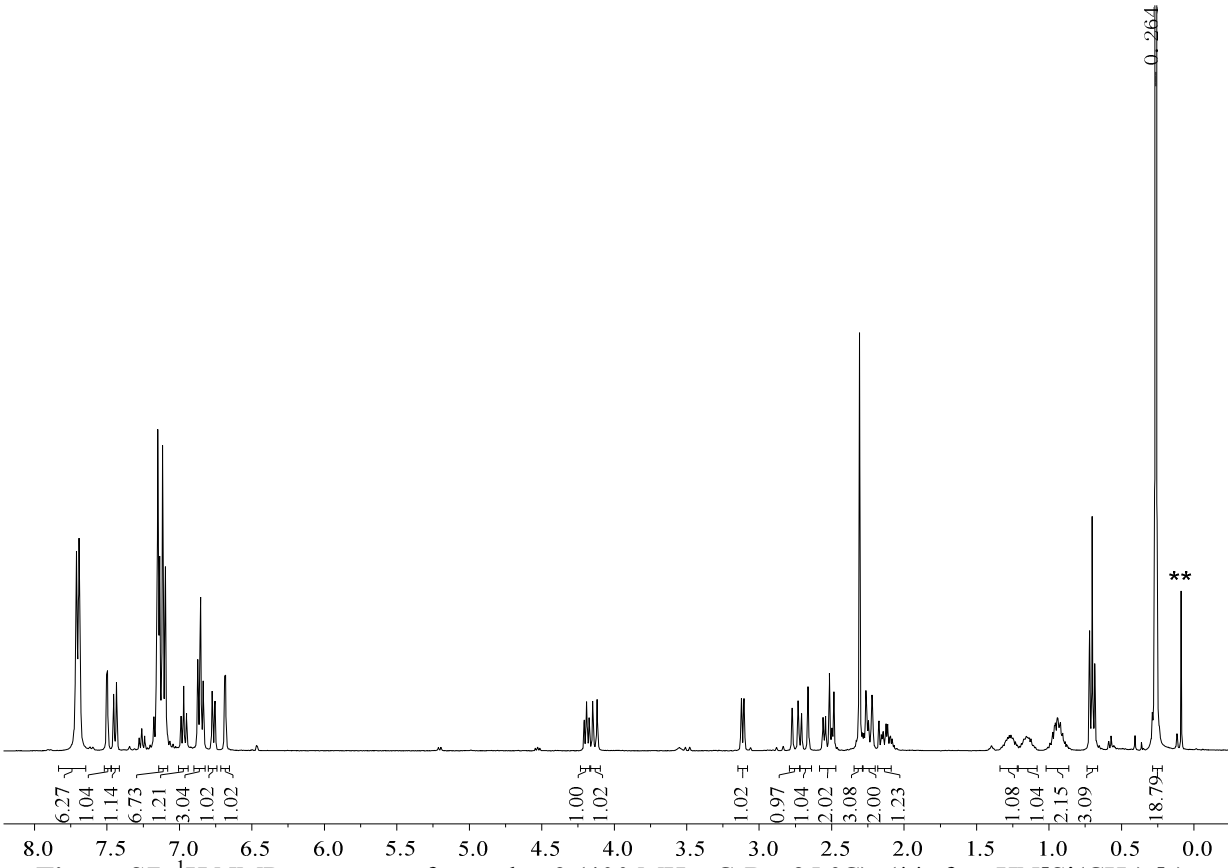

Figure S7. ^{1}H NMR spectrum of complex **2** (400 MHz, C_6D_6, 25 °C). (**: free $HN[Si(CH_3)_2]_2$).

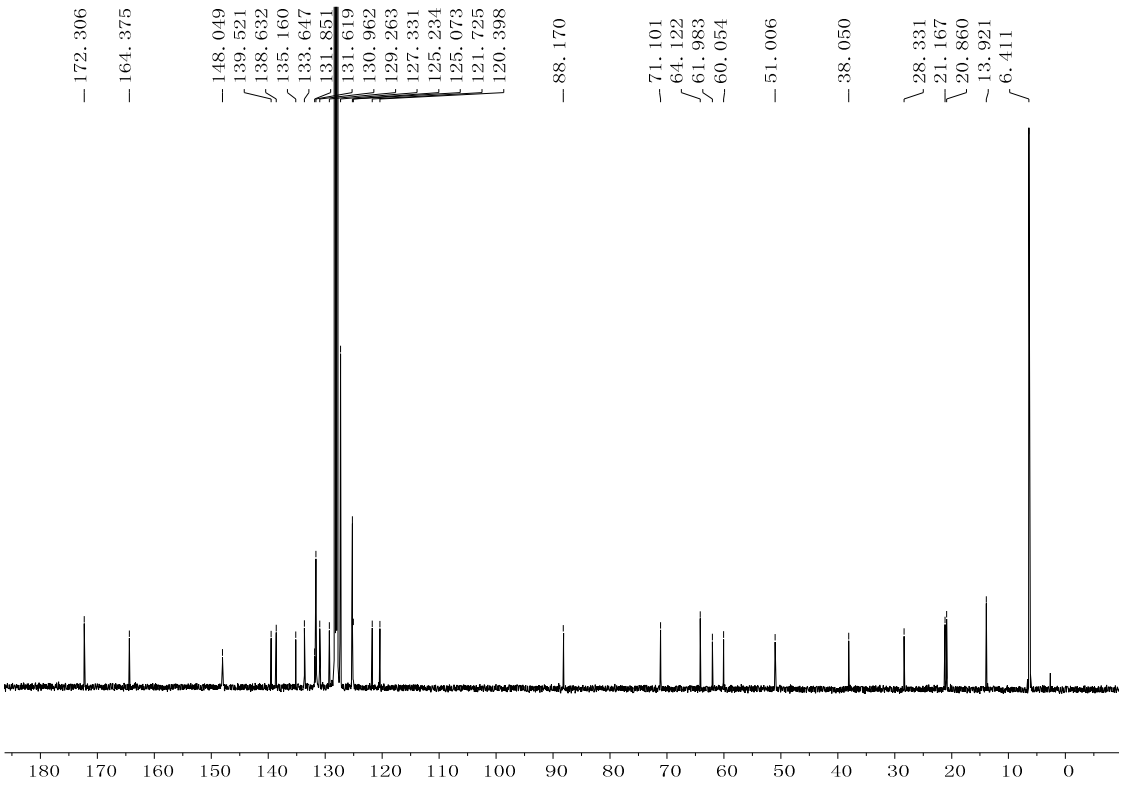

Figure S8. $^{13}C\{^{1}H\}$ NMR spectrum of complex **2** (100 MHz, C_6D_6, 25 °C).

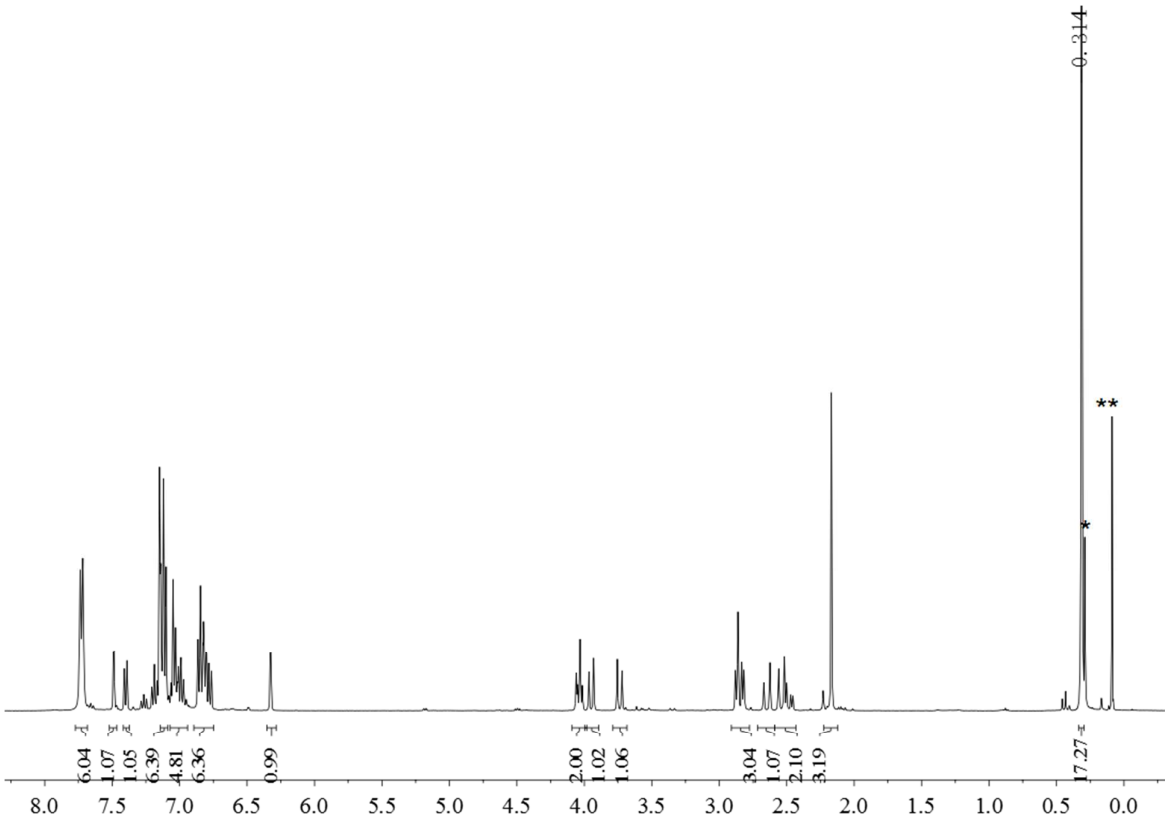

Figure S9. ^{1}H NMR spectrum of complex **3** (400 MHz, C_6D_6, 25 °C). (*: impurity in C_6D_6; **: free $HN[Si(CH_3)_2]_2$).

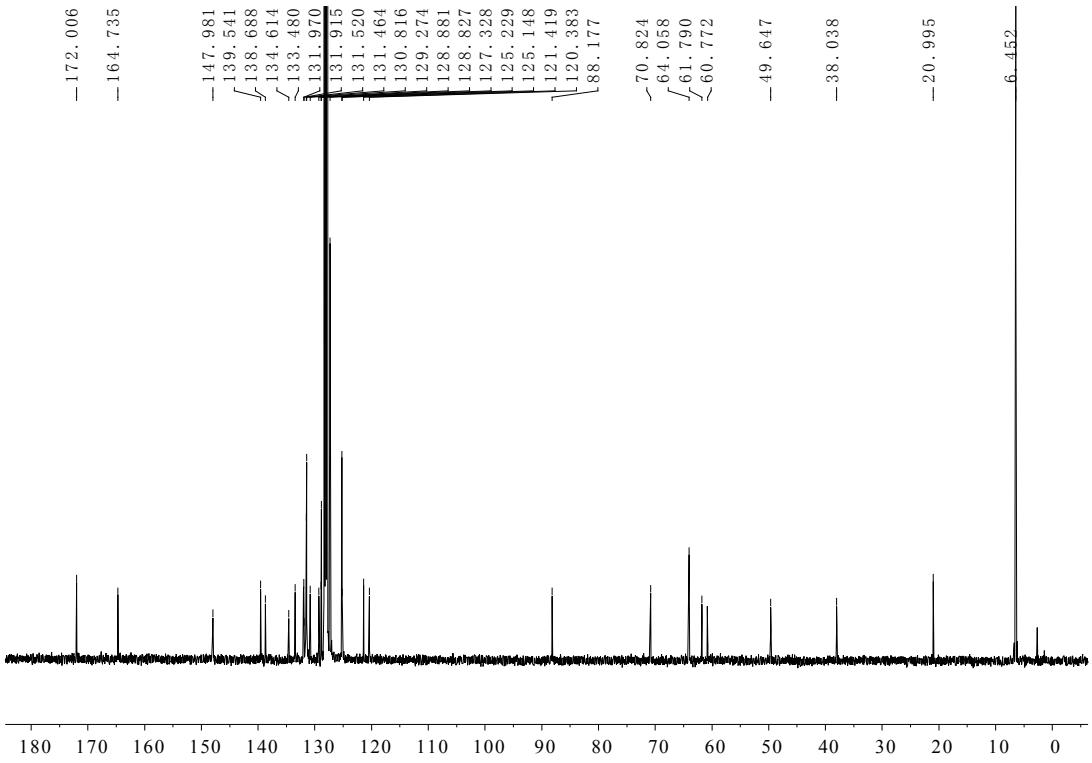

Figure S10. $^{13}C\{^{1}H\}$ NMR spectrum of complex **3** (100 MHz, C_6D_6, 25 °C).

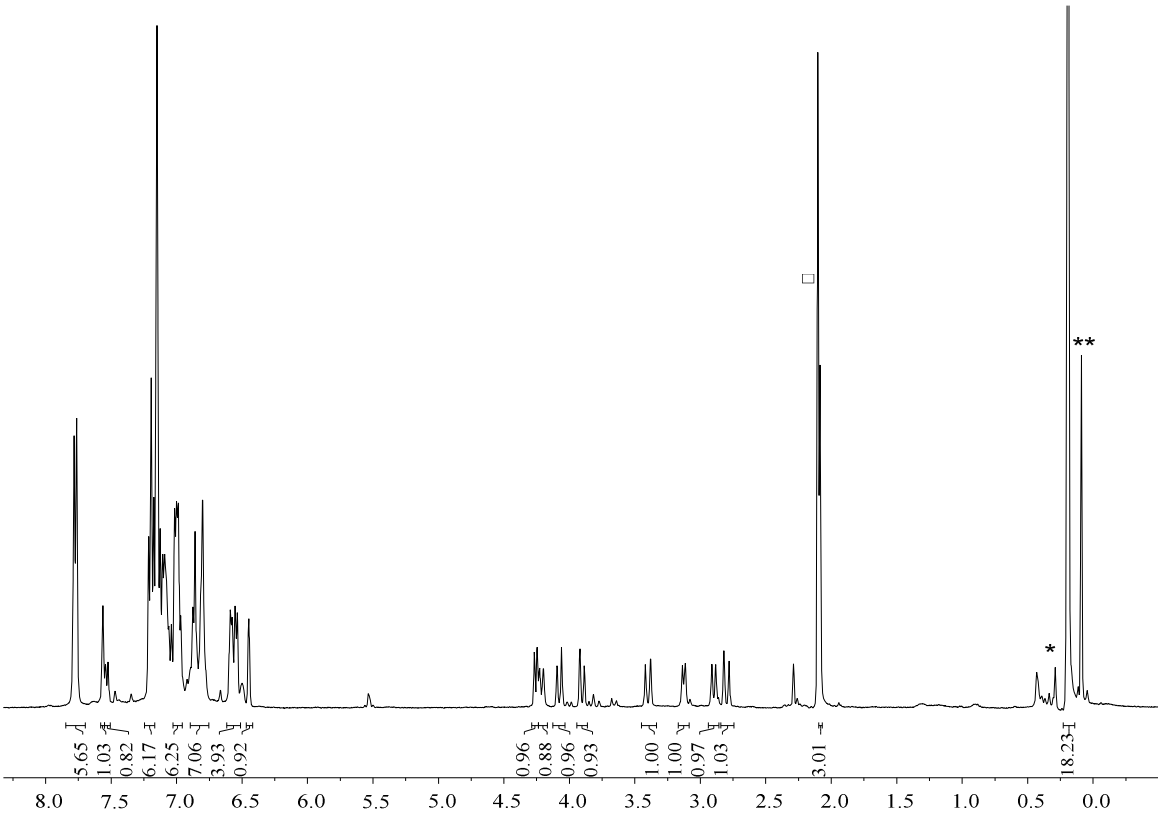

Figure S11. ^{1}H NMR spectrum of complex **4** (400 MHz, C_6D_6, 25 °C). (□: methyl signal of residual toluene; *: impurity in C_6D_6; **: free $HN[Si(CH_3)_2]_2$).

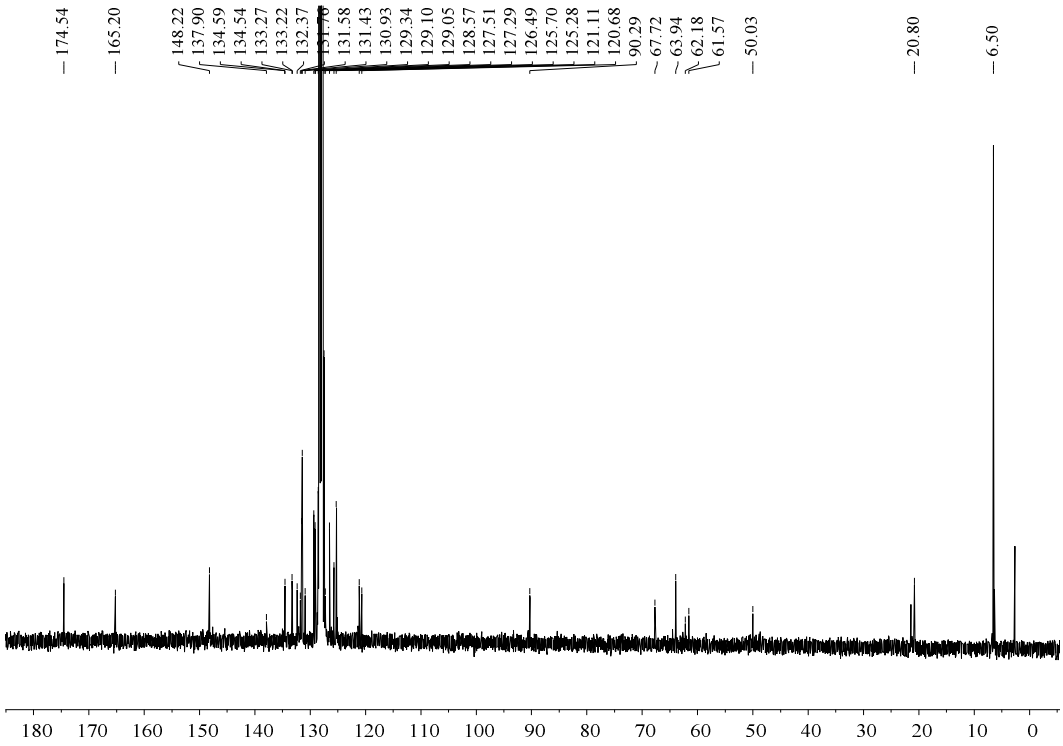

Figure S12. $^{13}C\{^{1}H\}$ NMR spectrum of complex **4** (100 MHz, C_6D_6, 25 °C).

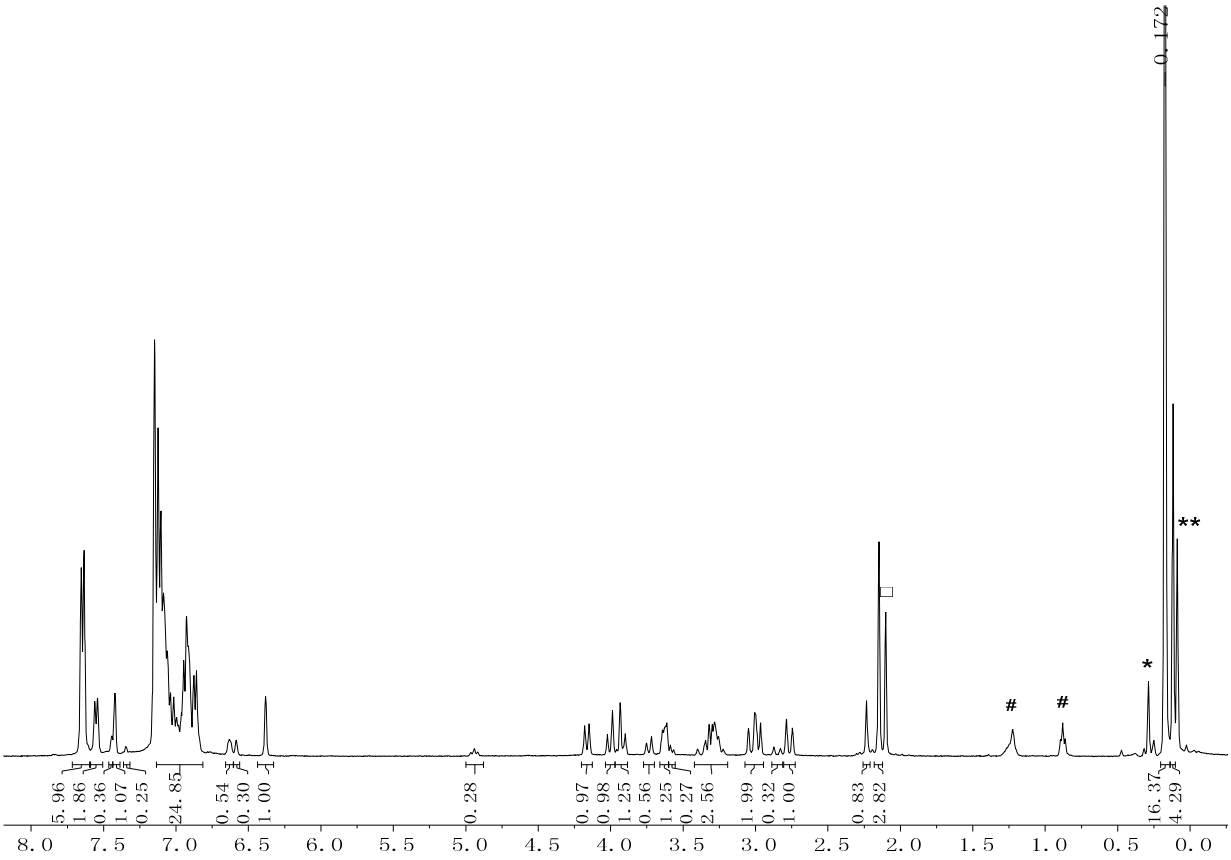

Figure S13. ^{1}H NMR spectrum of complex **5** (400 MHz, C_6D_6, 25 °C). (□: methyl signal of residual toluene; #: signals of *n*-hexane; *: impurity in C_6D_6; **: free $HN[Si(CH_3)_2]_2$).

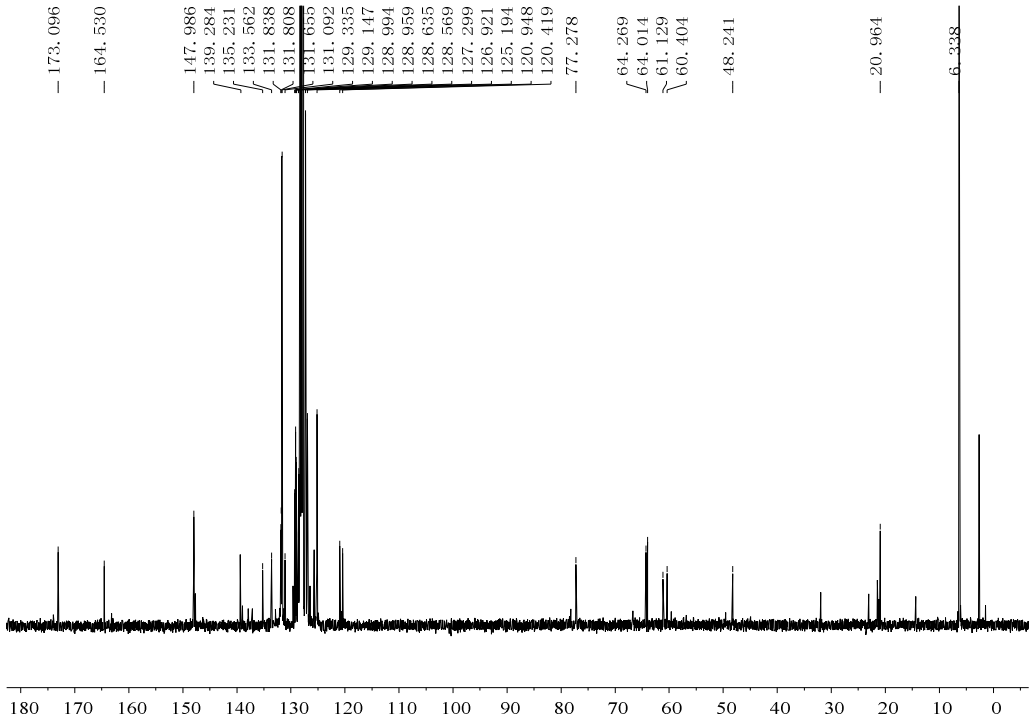

Figure S14. $^{13}C\{^{1}H\}$ NMR spectrum of complex **5** (100 MHz, C_6D_6, 25 °C).

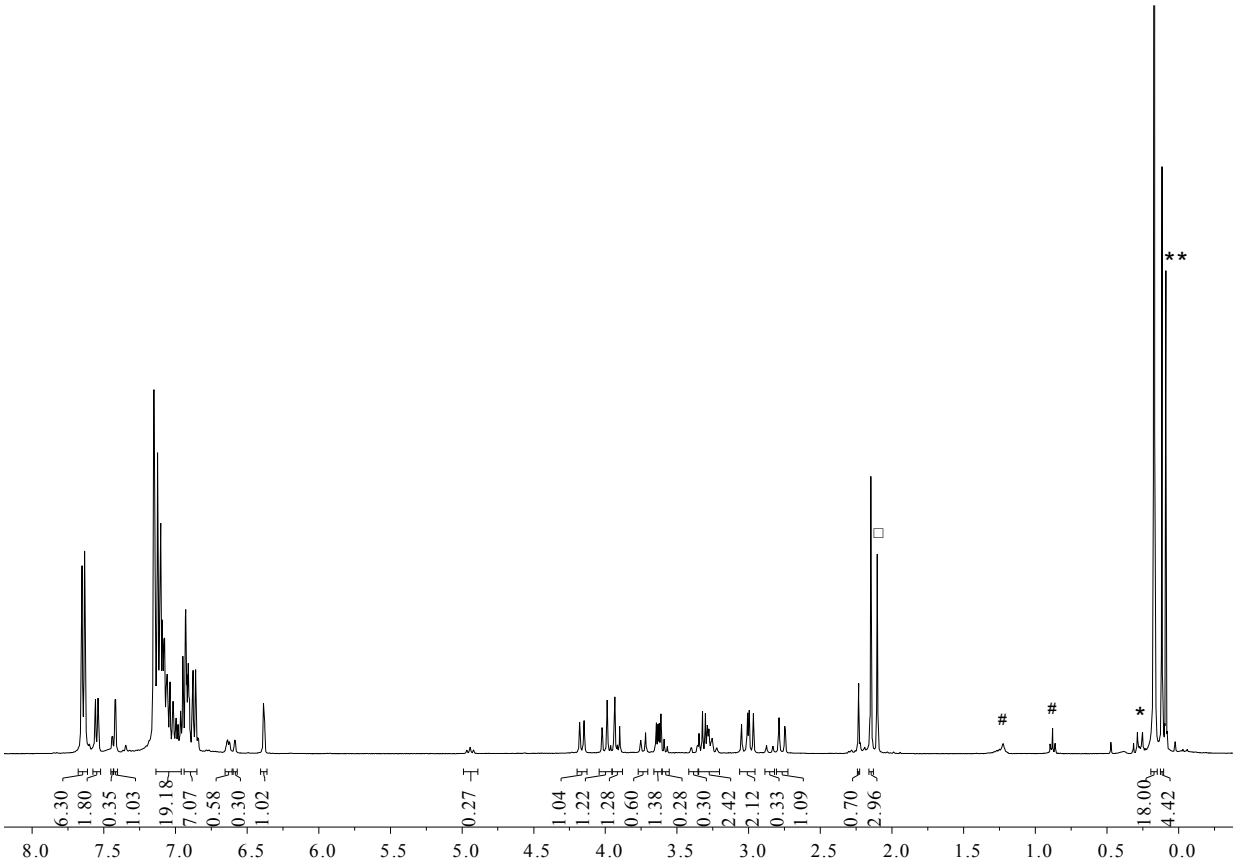

Figure S15. ^{1}H NMR spectrum of complex **6** (400 MHz, C_6D_6, 25 °C). (□: methyl signal of residual toluene; #: signals of *n*-hexane; *: impurity in C_6D_6; **: free $HN[Si(CH_3)_2]_2$).

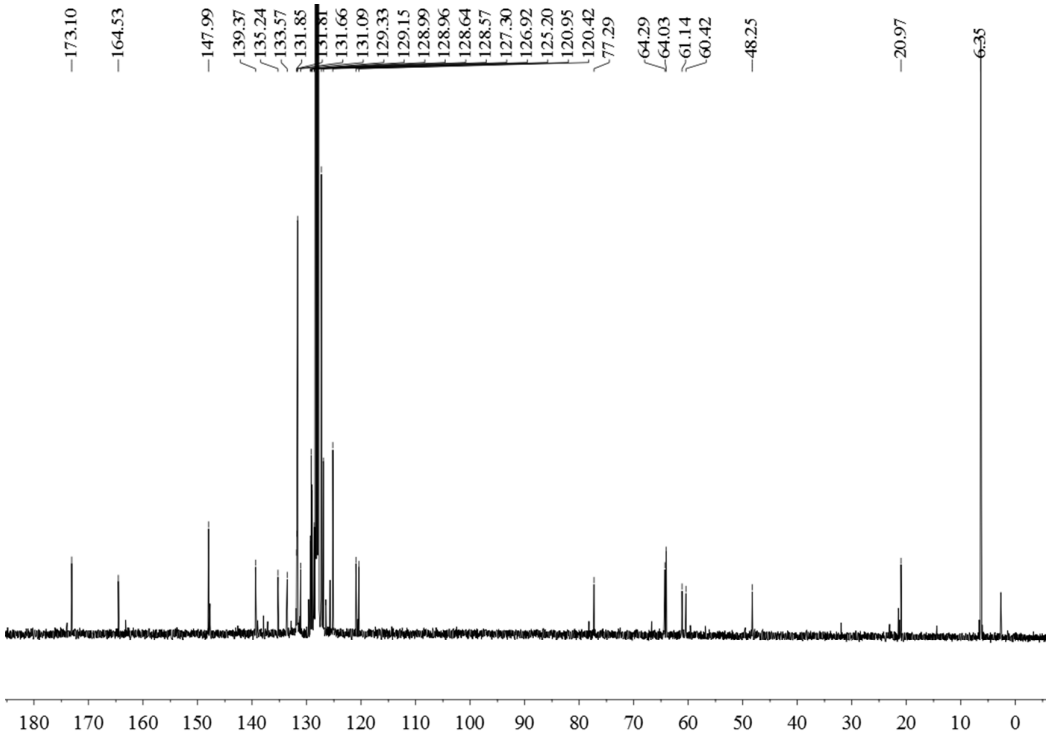

Figure S16. $^{13}C\{^{1}H\}$ NMR spectrum of complex **6** (100 MHz, C_6D_6, 25 °C).

2.3 Ring-opening polymerization, kinetic studies and microstructure analysis of poly(*rac*-lactide)

Table S2. ROP of *rac*-LA initiated by complexes **1-6**.[a]

Run	Cat.	Feed ratio	Time (min)	Conv.[b] (%)	$M_{n,calcd}$[c] ($\times 10^4$)	M_n[d] ($\times 10^4$)	M_w/M_n[d]	P_m[e]
1	**1**	500:1:0	19	91	6.55	8.90	1.68	0.47
2		500:1:1	8	90	6.48	6.44	1.37	0.48
3	**2**	500:1:0	6	90	6.48	9.35	1.56	0.54
4		500:1:1	2	96	6.91	6.28	1.32	0.55
5	**3**	500:1:0	22	86	6.19	16.2	1.46	0.52
6		500:1:1	15	91	6.55	8.61	1.24	0.51
7	**4**	500:1:0	16	90	6.48	9.12	1.67	0.52
8		500:1:1	5	93	6.70	6.73	1.36	0.51
9	**5**	500:1:0	26	90	6.48	8.21	1.62	0.51
10		500:1:1	15	88	6.34	6.95	1.33	0.50
11	**6**	500:1:0	25	91	6.55	7.21	1.60	0.50
12		500:1:1	15	90	6.48	6.43	1.39	0.50

[a] $[LA]_0$ = 1.0 M, THF, feed ratio = $[LA]_0/[Mg]_0/[^i PrOH]_0$, 25°C. [b] Determined by ^{1}H NMR spectroscopy. [c] $M_{n,calcd} = [LA]_0/[Mg]_0 \times$ Conv.% × 144.13 g/mol. [d] Determined by GPC. [e] The probability of forming a new *m*-dyad, determined by homonuclear decoupled ^{1}H NMR spectroscopy.

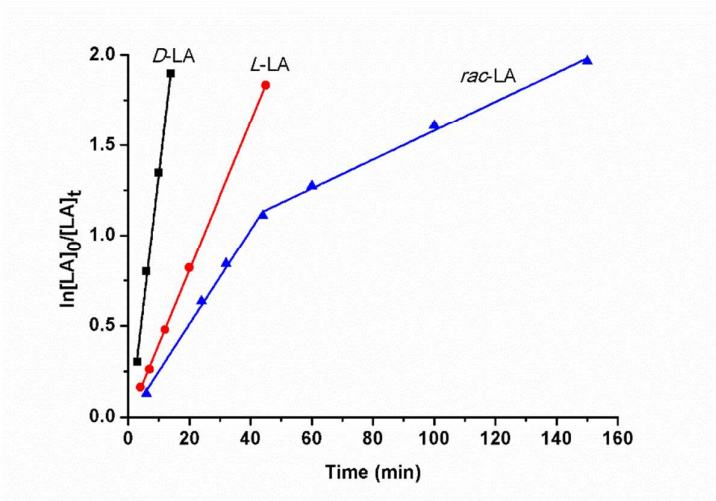

Figure S17. Plots of $\ln([LA]_0/[LA]_t)$ *vs* time for the ROP of *D*-LA, *L*-LA, and *rac*-LA catalyzed by **5**: $k_{app}(D)$ = (0.144 ± 0.004) min^{-1}, R = 0.997; $k_{app}(L)$ = (0.041 ± 0.001) min^{-1}, R = 0.999; $k_{app}^{1}(rac)$ = (0.028 ± 0.001) min^{-1}, R = 0.995; $k_{app}^{2}(rac)$ = (0.008 ± 0.0003) min^{-1}, R = 0.994; (0 °C, toluene, $[LA]_0/[^{i}PrOH]_0/[\mathbf{5}]_0$ = 750 : 1 : 1, $[LA]_0$ = 0.33 M).

In the case of *rac*-LA polymerization with complex **5**, the k_{app} is no more constant during the whole polymerization process and a kinetic plot with two approximate linear stages and a short curved transition was obtained. In the first approximation stage, the corresponding K_{app}^{1} is about (0.028 ± 0.001) min^{-1}, lower than that of *L*-LA (mismatched monomer) polymerization; in the second approximation stage, the K_{app}^{2} is about (0.008 ± 0.0003) min^{-1}, also lower than the half of that of *L*-LA polymerization, but the ratio of K_{app}^{1}/K_{app}^{2} is ca. 3.5. It seems that in both stages the propagation of polymer chains is retarded, that is, it the first stage the coordination-insertion of the matched monomer (*D*-LA) is significantly retarded due to the presence of the mismatched monomer (*L*-LA), and meanwhile the coordination-insertion of the mismatched monomer (*L*-LA) in the second stage is also retarded due to the presence of the matched monomer (*D*-LA) (considering moderate isoselectivity of P_m = 0.75). This is a quite unusual situation, and a competitive coordination of the mismatched monomer to the active center is not enough to explain it. Taking into account the dinuclear nature of the active species, we therefore suggest that the retardation in the whole polymerization period of *rac*-LA with complex **5** might be attributed to the formation of heteropropagation species (dimeric species bridged by two active polymer chains with ring-opened *D*- and *L*-LA as the latest inserted monomer respectively, denoted as Mg-*D*-*L*-Mg), which are probably either dormant states or much less active than the homopropagation species (dimeric species bridged by two active polymer chains with ring-opened *D*-LA or *L*-LA as the latest inserted monomers, denoted as Mg-*D*-*D*-Mg and Mg-*L*-*L*-Mg) due to the unfavorable coordination configuration for either *L*- or *D*-LA.

Peak	Integration	P_m
rmr	0.06	0.66
rmm	0.09	0.72
mmr	0.06	0.86
mmm	0.66	0.75
mrm	0.13	0.74
	Average	0.74

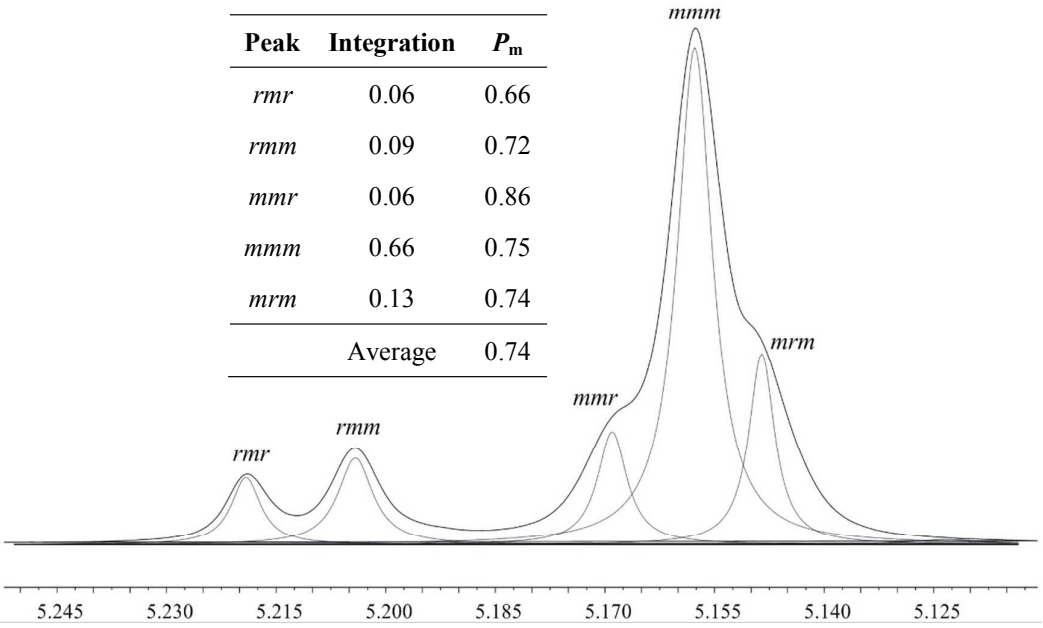

Figure S18. Methine region of the homonuclear decoupled ^{1}H NMR spectrum of isotactic PLA produced by using **5** as initiator ($[LA]_0$: $[Mg]_0$: $[^iPrOH]_0$ = 500 : 1 : 1, $[LA]_0$ = 1.0 M, in Tol at 25 °C).

Peak	Integration	P_m
rmr	0.05	0.68
rmm	0.06	0.85
mmr	0.07	0.84
mmm	0.71	0.79
mrm	0.11	0.78
	Average	0.78

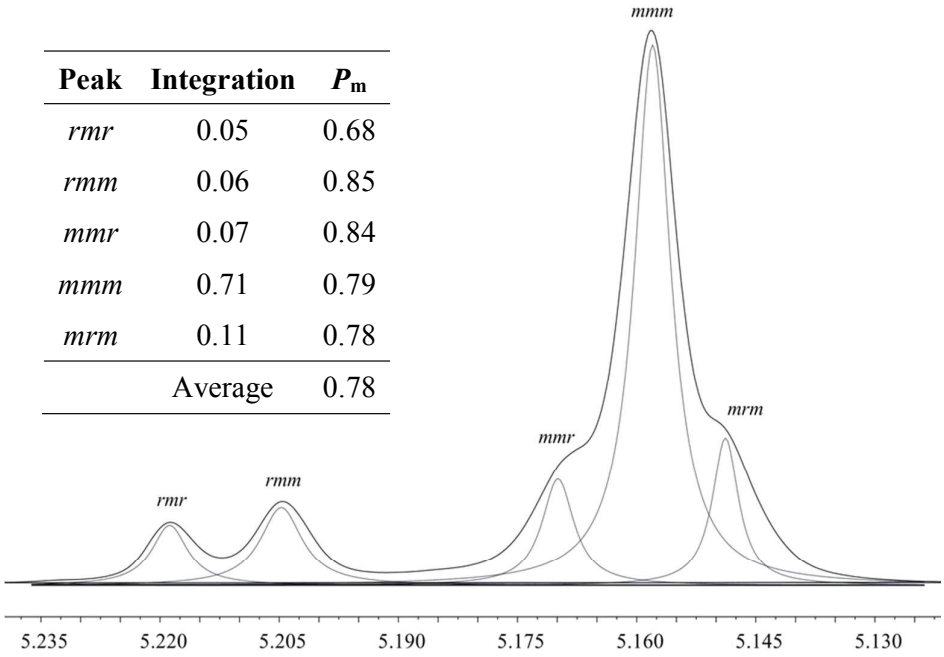

Figure S19. Methine region of the homonuclear decoupled ^{1}H NMR spectrum of isotactic PLA produced by using **5** as initiator ($[LA]_0$: $[Mg]_0$: $[^iPrOH]_0$ = 500 : 1 : 0, $[LA]_0$ = 1.0 M, in Tol at –40 °C).

Peak	Integration	P_m
rmr	0.03	0.78
rmm	0.08	0.74
mmr	0.07	0.78
mmm	0.74	0.82
mrm	0.08	0.86
	Average	0.80

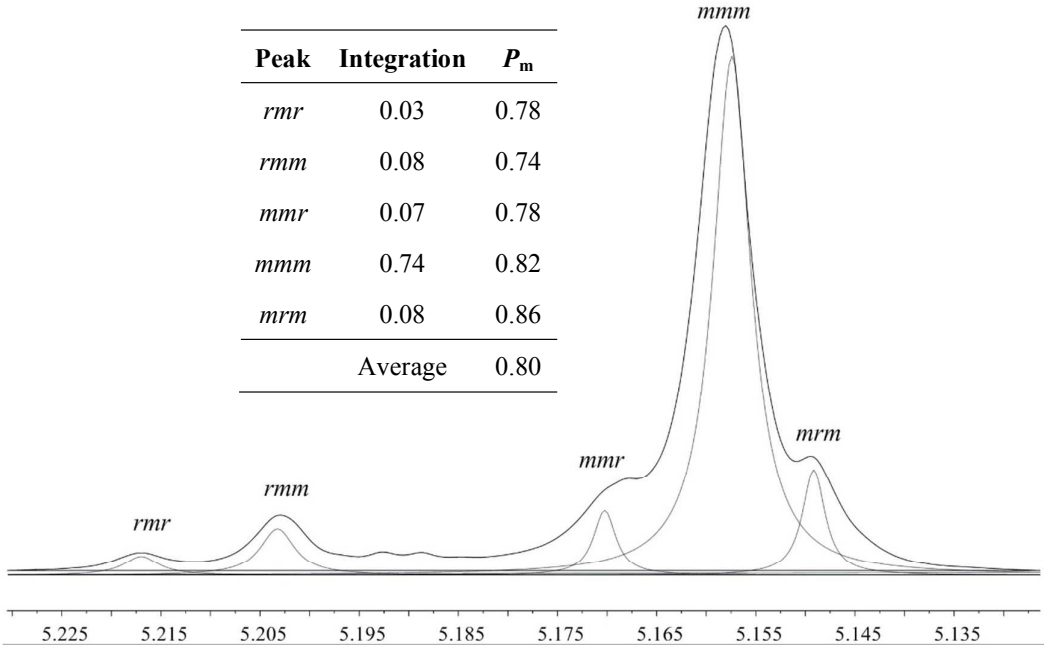

Figure S20. Methine region of the homonuclear decoupled ^{1}H NMR spectrum of isotactic PLA produced by using the mixture of **5** and **6** as initiator ($[LA]_0$: $[Mg]_0$: $[^iPrOH]_0$ = 1000 : 1 : 1, $[LA]_0$ = 1.0 M, in Tol at 25 °C).

Peak	Integration	P_m
rmr	0.02	0.79
rmm	0.06	0.86
mmr	0.06	0.85
mmm	0.79	0.85
mrm	0.07	0.86
	Average	0.84

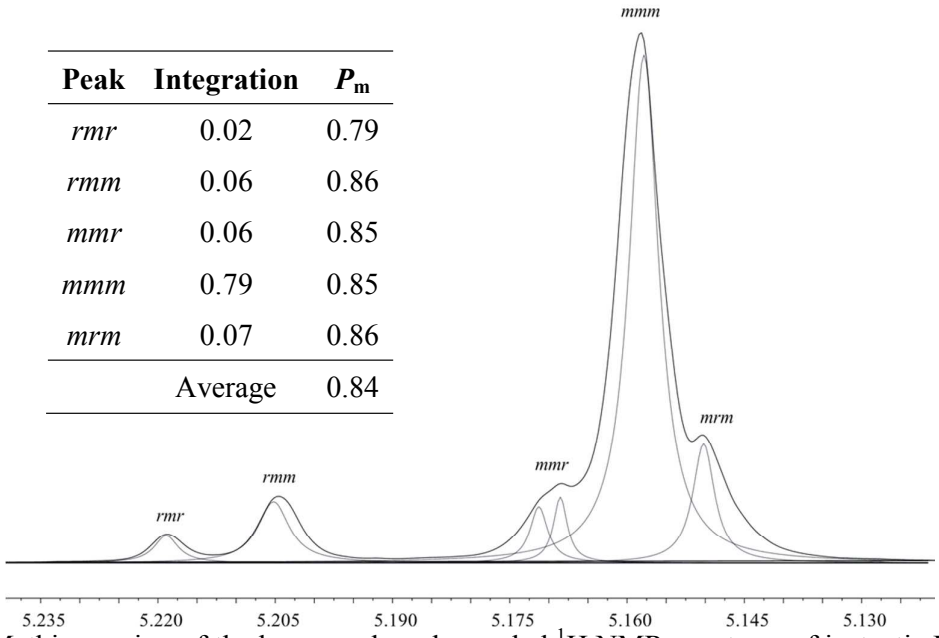

Figure S21. Methine region of the homonuclear decoupled ^{1}H NMR spectrum of isotactic PLA produced by using the mixture of **5** and **6** as initiator ($[LA]_0$: $[Mg]_0$: $[^iPrOH]_0$ = 500 : 1 : 0, $[LA]_0$ = 1.0 M, in Tol at –40 °C).

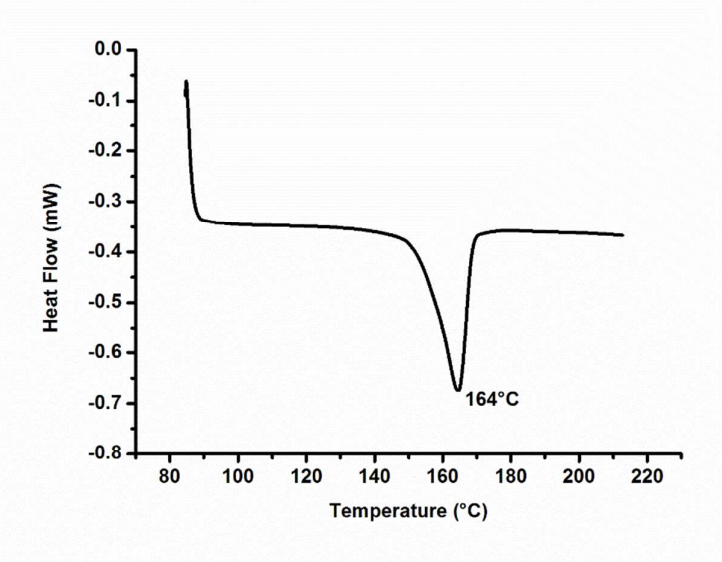

Figure S22. Heat flow *vs.* temperature curve of PLA obtained from *rac*-LA by using the mixture of **5** and **6** (P_m = 0.80) as initiator at 25 °C.

Reference

[S1] H. Bürger, W. Sawodny, U. Wannagat, *J. Organomet. Chem.* **1965**, *3*, 113.

[S2] Kan, C.; Hu, J.; Huang, Y.; Wang, H.; Ma, H. Highly Isoselective and Active Zinc Catalysts for *rac*-Lactide Polymerization: Effect of Pendant Groups of Aminophenolate Ligands. *Macromolecules* **2017**, *50*, 7911–7919.

[S3] H. Ammar, B. Hassine, C. Fischmeister, P. Dixneuf, C. Bruneau, *Eur. J. Inorg. Chem.* **2010**, 4752.

[S4] a) J. F. Larrow, E. N. Jacobsen, Y. Gao, Y. Hong, X. Nie, C. M. Zepp, *J. Org. Chem.* **1994**, *59*, 1939; b) M. Huang, C. Pan, H. Ma, *Dalton Trans.* **2015**, *44*, 12420.

[S5] *SADABS*, Bruker Nonius area detector scaling and absorption correction, V2.05, Bruker AXS Inc., Madison, WI, **1996**.

[S6] G. M. Sheldrick, SHELXTL 5.10 for windows NT, Structure Determination Software Programs, Bruker Analytical X-ray Systems, Inc., Madison, WI, **1997**.

[S7] SAINT, Version 6.02, Bruker AXS Inc., Madison, WI, **1999**.

[S8] G. M. Sheldrick, SHELXS-97, Program for the Solution of Crystal Structures, University of Göttingen, Germany, **1990**.

[S9] G. M. Sheldrick, *SHELXL-97*, Program for the Refinement of Crystal Structures, University of Göttingen, Germany, **1997**.

[S10] L. J. Farrugia, *J. Appl. Crystallogr.* 1997, **30**, 565; ORTEP-III for Windows-Version 2.0, University of Glasgow, **2008**.